Eur. Phys. J. D **6**, 283–290 (1999)

THE EUROPEAN PHYSICAL JOURNAL D

EDP Sciences

Far-field fluorescence microscopy with repetitive excitation

A. Schönle and S.W. Hell[a]

High Resolution Optical Microscopy Group, Max-Planck-Institute for Biophysical Chemistry
37070 Göttingen, Germany

Received: 3 December 1998

Abstract. We introduce the concept of repeatedly exciting an excited state of a photostable fluorescent entity to generate a nonlinear fluorescence signal which is solely based on the linear susceptibility of the molecule. The excitation cycle between the fluorescent state S_1 and another state prolongs the average lifetime of S_1, with emphasis on those molecules that are in the center of the focus. The photons emitted by the long-lived molecules in the center are recorded by a temporal filter and constitute fluorescence that depends nonlinearly on the excitation intensity. Theoretical analysis reveals that this concept can provide three-dimensional imaging and improve the spatial resolution in far-field fluorescence microscopy. We show that despite the presence of diffraction the effective focal waist can in principle be narrowed down to the molecular scale at the expense of signal.

PACS. 42.90.+m Other topics in optics – 42.30.-d Imaging and optical processing – 42.65.-k Nonlinear optics

1 Introduction and motivation

In spite of the success of electron and scanning tip microscopes, far-field light microscopy has maintained its dominant role in biological imaging. This is due to the unique ability of focused light to penetrate a cell and to image the cell interior. Confocal and multiphoton scanning microscopes routinely produce three-dimensional (3D) images from cells and tissue with a resolution up to about 200 and 600 nm in the lateral and axial direction, respectively [1].

Confocal and multiphoton microscopes are able to deliver 3D images because their effective point-spread-function (E-PSF) depends nonlinearly on the focal illumination intensity given mathematically by the illumination PSF (I-PSF). The nonlinearity confines the E-PSF around the focal point so that the E-PSF acts as a 3D probe with which the sample is probed in a raster fashion. In fact, nonresonant two- [2] and three-photon [3] excitation of fluorescence is an elegant approach to obtain a spatially confined 3D EPSF that has enjoyed routine implementation in scanning microscopy.

Due to the quadratic and cubic dependence of the fluorescence on the excitation intensity, nonresonant two- and three-photon excitation are sometimes cited to improve the spatial resolution of a scanning microscope. This is because the nonlinear dependence suppresses the outer regions of the I-PSF thus rendering an E-PSF that is compressed with respect to the latter. However, this is not evident since multiphoton excitation of visible fluorescence usually requires recourse to a doubled and tripled wavelength. This brings about doubling or tripling of the spatial extent of the I-PSF which cannot be fully compensated for by the shrinkage induced by the nonlinearity. As a result, the resolution of a multiphoton microscope is generally poorer than that of its single-photon scanning counterpart [4]. Applying a shorter wavelength and direct nonresonant multiphoton excitation to a higher state is generally no solution because of the concomitant potential single-photon excitation to the first state. Inducing fluorescence from a higher-lying state, for example by stepwise two-photon excitation, would improve the resolution [5], however, higher-state fluorescence is reportedly exceptional [6]. Transient absorption of the excited state has been reported to add optical sectioning capabilities to an absorption (transmission mode) microscope [7], however, it does not lead to a significant resolution improvement in general. Nevertheless, exploiting nonlinearities to fundamentally improve the spatial resolution of a far-field microscope deserves further investigation. In this paper, we introduce and investigate the concept of repetitive excitation of a fluorophore to obtain 3D images and higher spatial resolution in fluorescence microscopy.

2 Concept

The basic idea can be explained as follows. Imagine an organic fluorophore with its states arranged as in Figure 1. It is excited by an initial pulse from the ground state to the first singlet state, $S_0 \rightarrow S_1$ (Fig. 2a). The latter state would usually decay to the ground state within a

[a] e-mail: shell@gwdg.de

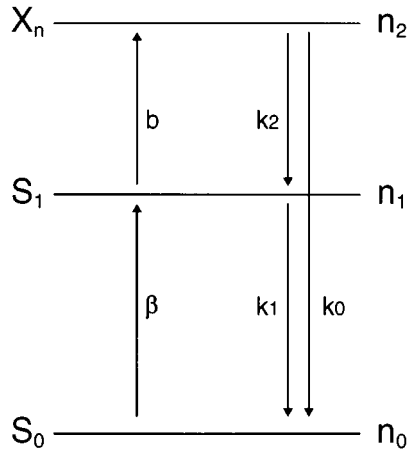

Fig. 1. Energy state (Jablonski) diagram of our model dye. The state X_n can be any photostable state decaying mainly into the first excited singlet state. The parameters β and b denote the pump rates due to the first and second laser source.

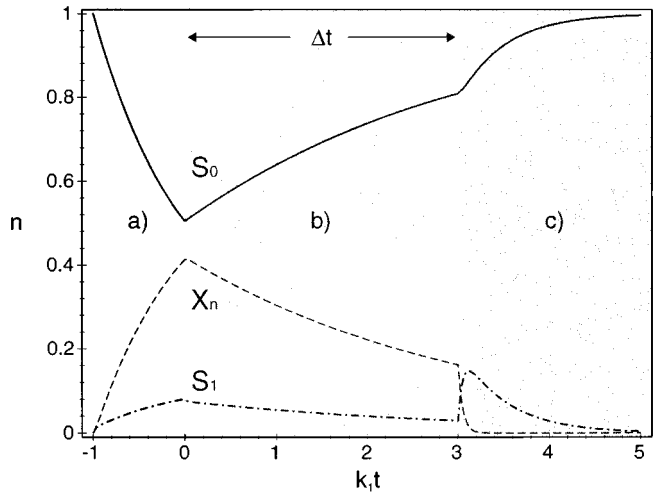

Fig. 2. Time scheme of repetitive excitation. During the initial phase a) the dye is excited by the first laser beam to its first excited state S_1 and further excited into the state X_n by the second (re-excitatory) laser. During phase b) the first laser is off and the molecule decays into its ground state at a slower rate than k_1 due to the re-excitatory laser. After a time window Δt this laser, too, is switched off and all dyes in state X_n drop into their first excited state. Further decay during phase c) into the ground state is at a faster rate k_1. The fluorescence produced during this phase is detected.

few nanoseconds whereby a fluorescent photon is emitted. Let us now assume that the molecule is also exposed to a *second* pulse (Fig. 2a, b) incapable of inducing the excitation $S_0 \rightarrow S_1$ but capable of transferring the molecule from S_1 to a higher state X_n. From X_n the molecule decays back to the fluorescent state S_1 within several picoseconds. The state X_n could be any higher-energy state S_n, that ideally fulfils the requirements of photostability and a dominant relaxation $X_n \rightarrow S_1$ into the fluorescent state.

Due to the small but finite lifetime of the state X_n, the cycle $S_1 \rightarrow X_n \rightarrow S_1$ artificially prolongs the lifetime of the fluorescent decay $S_1 \rightarrow S_0$. Repetition of the cycle $S_1 \rightarrow X_n \rightarrow S_1$ by multiple absorption of a photon of the second pulse is expected to substantially increase the lifetime. The more photons a molecule has absorbed the longer is the effective lifetime of the fluorescence decay to the ground state. A reduced population of S_1 brought about by absorption of intense laser radiation was made responsible for the fluorescence quenching observed in some laser dyes [8].

The consequences of repeated excitation on the effective PSF of a scanning microscope are readily envisaged. Repeated excitation keeps the molecules in the closest vicinity of the focal point in the cycle whereas those of the outer part of the focus drop down to the ground state. This stems from the fact that molecules in the focal center have a higher probability of repeated excitation than those at the edge of the focus. After a certain time span Δt, the irradiation ends and the remaining fluorescence is detected (Fig. 2). Using this technique, repeated excitation at the *same* excitation wavelength is able to sharpen the effective PSF in all directions. It is thus conceivable that one could continuously increase the order of excitation and shrink the 3D PSF simply by applying a sufficiently long second pulse and waiting long enough. Thus one could think of achieving — at a marked loss of signal but without infringing the laws of diffraction — far-field microscopy resolution at the molecular scale.

In practice, the resolution and the contrast in the image will be co-determined by the achievable signal and therefore by the photophysical and photochemical properties of the fluorescent system. The attainable signal will determine whether the concept can be employed for a marked resolution improvement or for 3D imaging. So far, organic fluorophores have been mostly used as fluorescence emitters leading us to evaluate the concept of repetitive excitation for systems analogous to organic molecules. However, the underlying principle is valid for any light-emitting system fulfilling the excitation and emission properties below.

3 Nonlinearity through repetitive excitation

For light pulse durations of the order of a nanosecond and not too intense pulses the vibronic sub-states of the electronic states S_i can be largely ignored [6,8]. Therefore the interplay between light and the various electronic states of an organic molecule during the second pulse is described by a set of linear differential equations

$$\frac{\mathrm{d}}{\mathrm{d}t}\begin{pmatrix} n_0 \\ n_1 \\ n_2 \end{pmatrix} = \begin{pmatrix} -\beta & k_1 & k_0 \\ \beta & -k_1 - b & k_2 \\ 0 & b & -k_2 - k_0 \end{pmatrix} \begin{pmatrix} n_0 \\ n_1 \\ n_2 \end{pmatrix}, \qquad (1)$$

with n_i representing the population of the state S_i. The populations $n_i \equiv n_i(t)$ are functions of time and their temporal evolution is governed by the excitation rates β and b, which are proportional to the photon flux per area of the first and second pulse, respectively. The variables k_j denote the transition rates per molecule per second

for the various relaxations as depicted in Figure 1. In order to describe accurately the process of initial excitation through the first pulse as shown in Figure 2, a general solution of the above equation is required [8]. For all following calculations we note that for moderate pump rates the probability of a molecule to be excited directly after the pulse depends approximately linearly on β. For the description of the time evolution during the second part of the process we set $\beta = 0$ in equation (1) and are left with only two relevant equations:

$$\frac{\mathrm{d}}{\mathrm{d}t}\begin{pmatrix} n_1 \\ n_2 \end{pmatrix} = -\begin{pmatrix} k_1 + b & -k_2 \\ -b & k_2 + k_0 \end{pmatrix}\begin{pmatrix} n_1 \\ n_2 \end{pmatrix} . \tag{2}$$

The value for n_0 always follows from the normalisation $\sum_i n_i = 1$. Let the excitation of X_n end a time Δt later than that of S_1. During the rest of the cycle the remaining fluorescence should be collected. The fluorescence signal is proportional to the total probability of the dye to be still excited after the second pulse ends, which is given by $\eta(b, \Delta t) = n_1(\Delta t) + n_2(\Delta t)$. Based on the above considerations we expect $\eta(b, \Delta t)$ to be a nonlinear function of b. In order to establish the nonlinearity, we write $x = \ln(b/A)$ and define the variable

$$\gamma(b, \Delta t) = \left.\frac{\mathrm{d}}{\mathrm{d}x}\ln(\eta(A\exp(x), \Delta t))\right|_{x=\ln(\frac{b}{A})} = \frac{b}{\eta(b, \Delta t)}\frac{\mathrm{d}}{\mathrm{d}b}\eta(b, \Delta t) \tag{3}$$

representing the slope of a double-logarithmic plot. A is an arbitrary constant of the same dimension as b. The variable $\gamma(b, \Delta t)$ quantifies the nonlinearity of the fluorescence as a function of the excitation power.

For very low excitation intensities of the second (re-excitatory) pulse, $b \to 0$, we expect $\gamma(b, \Delta t) \to 0$, since the effect of the repetitive excitation vanishes. Likewise, for very high excitation intensities, $b \to \infty$, we can also expect $\gamma(b, \Delta t) \to 0$ since saturation of the upper excited state, X_n, flattens out any dependence of the fluorescence on the power of the re-excitatory pulse. $\gamma(b, \Delta t)$ will therefore reach a global maximum $\gamma_{\max}(\Delta t)$ which will be the upper bound for the achievable nonlinearity.

In order to obtain an initial insight into operational parameters of this concept, we calculate $\gamma_{\max}(t)$. By assuming weak relaxation $X_n \to S_0$ and that the nonradiative relaxation $X_n \to S_1$ is much faster than the fluorescence relaxation $S_1 \to S_0$, $k_0 \ll k_1 \ll k_2$, which is a reasonable assumption, we can derive an analytical expression for $\gamma_{\max}(t)$. In this case the change of the population of excited molecules is simply the change of the population in the first excited state:

$$\frac{\mathrm{d}}{\mathrm{d}t}\eta = -k_1 n_1 . \tag{4}$$

Since $k_1 \ll k_2$, the excitation of S_1 with the second pulse leads to a transient equilibrium between S_1 and S_2. Hence, we obtain in good approximation

$$k_2 n_2 = b n_1 \quad \text{and} \quad n_1 = \frac{k_2}{k_2 + b}\eta . \tag{5}$$

Substitution of (5) into (4) leads to

$$\frac{\mathrm{d}}{\mathrm{d}t}\eta = -\frac{k_2}{k_2 + b}k_1\eta \tag{6}$$

and finally to

$$\eta(b, t) = \exp\left(-\frac{k_2}{k_2 + b}k_1 t\right) , \tag{7a}$$

$$\gamma(b, t) = \frac{k_2 b}{(k_2 + b)^2}k_1 t . \tag{7b}$$

The function $\gamma(b, t)$ vanishes for low and for high excitation intensities b, as predicted. Moreover, we find a global nonlinearity maximum at the photon flux $b = k_2$, that is the pump rate equals the decay rate of the higher-lying excited state. At this excitation intensity, the maximum nonlinearity is given by

$$\gamma_{\max}(b, t) \equiv \tau = \frac{1}{4}k_1 t , \tag{8}$$

revealing that the nonlinearity increases with time. This is an interesting result as it indicates that the nonlinearity of the signal can be continuously increased by using a long enough re-excitatory pulse and by filtering out photons that are emitted after a long enough time span.

However, temporal filtering and the concomitant increase in nonlinearity is accompanied by a reduced signal. Therefore, we calculate the reduction of the fluorescence signal as a function of the nonlinearity. This is found by substituting t by γ in the expression for the population of the excited state:

$$\eta(b, \gamma) = \exp\left(-\gamma\frac{k_2 + b}{b}\right) . \tag{9}$$

We find that the population and hence the fluorescence yield decreases exponentially with nonlinearity; at $b = k_2$ we obtain $\eta(\gamma) = \exp(-2\gamma)$. Hence a quartic dependence $\gamma = 4$ would lead to a reduction of the maximum signal by a factor of 3×10^3 so that in a scanning microscope one would have to increase the pixel dwell time from the typical $\sim \mu$s to tens of ms. Our initial approximation yields that, although much higher nonlinearities are achievable for organic molecules in this concept, only values $1 \leq \gamma \leq 4$ appear to be in the practically useful range. These values are already sufficient for providing three-dimensional imaging or for significantly improving the resolution in three dimensions.

The intensities required for realising this concept are established by the absorption cross-sections and magnitude of the relaxation rates. The functionality of the concept of repetitive excitation relies only on the ratio between the various transitions. So far, we neglected k_0 and also assumed k_2 to be much larger than the fluorescence rate k_1. As both are reasonable assumptions they facilitated the description of the principles of the concept of repetitive excitation without affecting its main

conclusions. By introducing the variables $\theta = k_2/k_1$ and $\kappa = k_0/k_1$ we now investigate the effect of k_0 and k_2 and provide a more detailed solution of the problem: Defining $\vec{n} \equiv \begin{pmatrix} n_1 \\ n_2 \end{pmatrix}$ we formally write equation (2) as

$$\frac{\mathrm{d}}{\mathrm{d}t}\,\vec{n} = M\,\vec{n}$$

with the solution

$$\vec{n}\,(t) = \exp(Mt)\,\vec{n}\,(t=0)\,.$$

The eigenvalues of M are found as

$$\kappa_{1,2} = -\varsigma \pm \chi\,, \tag{10}$$

with

$$\begin{aligned} \varsigma &= \frac{1}{2}(k_0 + k_2 + k_1 + b)\,, \\ \chi &= \sqrt{\nu^2 + k_2 b}\,, \\ \nu &= \frac{1}{2}(k_0 + k_2 - k_1 - b)\,. \end{aligned} \tag{11}$$

We consider the time evolution for initially excited dyes. The initial population of the excited states after ending the excitation $S_0 \rightarrow S_1$ is then approximately given by

$$\vec{n}\,(t=0) = \frac{1}{k_2 + b}\begin{pmatrix} k_2 \\ b \end{pmatrix}$$

and the solution is found in a closed form:

$$\begin{aligned} \eta(b,t) = n_1(b,t) + n_2(b,t) &= \frac{[e^{\kappa_1 t} + e^{\kappa_2 t}]}{2} \\ &+ [2k_2 b + \nu(k_2 - b)]\frac{[e^{\kappa_1 t} - e^{\kappa_2 t}]}{2\chi(k_2 + b)}\,. \end{aligned} \tag{12}$$

Figure 3 shows the function $\eta(b, \Delta t)$ describing the relationship between the fluorescence signal and the intensity of the re-excitatory pulse. As a parameter we have chosen various delays $\Delta t = 4\tau/k_1$, *i.e.* various maximal nonlinearities $\tau \equiv \gamma_{\max}$. The evaluation was carried out for the values of $\theta = 0.1$ and $\kappa = 0.05$. The inlay shows the nonlinearity $\gamma(b,t)$ as a function of the re-excitatory pulse for the same photophysical conditions. The graphs clearly reveal a sub-linear and linear dependence for very high and low excitation intensity b and a strong nonlinear dependence at around $b = k_2$.

The effect of non-negligible decay $S_2 \rightarrow S_0$ is easy to predict since it can be regarded as a leak resulting in a reduced total signal. The consequences are also found in Figure 3: the maximum nonlinearity $\gamma_{\max}$ will be slightly lower than the maximum value τ obtained from equation (8) and it will be slightly offset from the excitation intensity $b = k_2$. Figure 4 explicitly examines the effect of an increasing "leak". Both offset and reduction of $\gamma_{\max}$ become large for values of $\kappa > 0.1$. Throughout the paper we assumed a value of $\kappa = 0.05$.

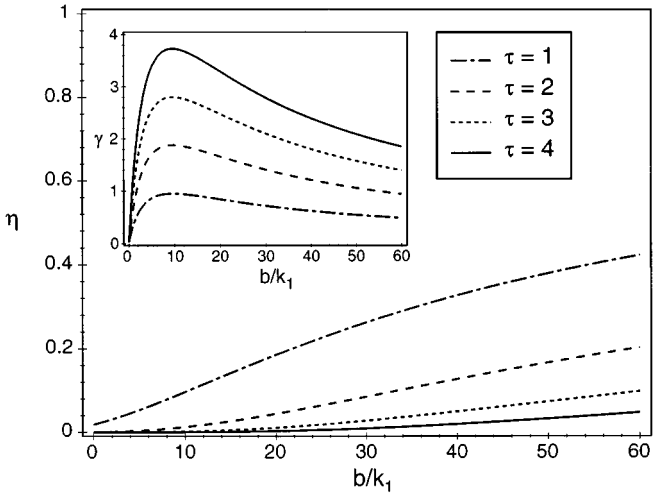

Fig. 3. The function $\eta(b, \Delta t)$ and the slope of its double logarithmic plot γ (inlay) for various values of the delay $\Delta t = 4\tau/k_1$. We chose $\theta = k_2/k_1 = 10$ and $\kappa = 0.05$ for this plot. The parameter τ indicates the maximum achievable nonlinearity at optimum parameter values. The nonlinearity has a maximum around $b = k_2$ and drops off for high and low values.

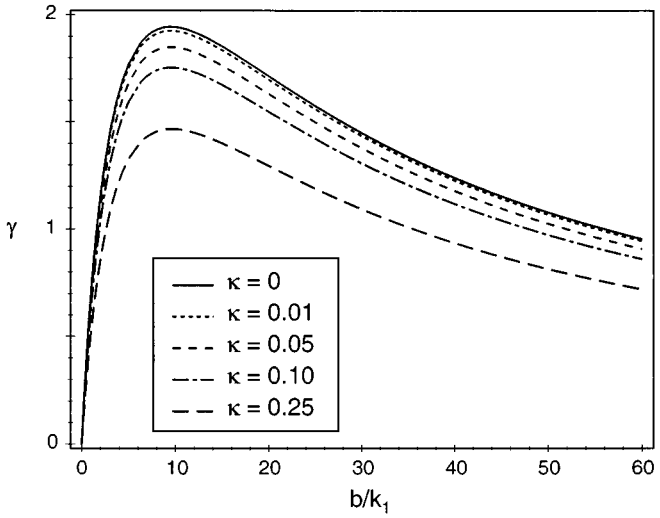

Fig. 4. The nonlinearity γ now for different rates κ of the transition $X_n \rightarrow S_0$. The delay corresponds to $\tau = 2$. For increasing leak rates the maximum nonlinearity becomes weaker and the maximum is slightly shifted to larger values of the pump rate.

4 Point-spread-function of a scanning microscope using repetitive excitation

Let r and z be cylindrical coordinates originating at the focal point and $\nu = k \times n \times \sin(\alpha) \times r$ and $u = 4k \times n \times \sin^2(\alpha/2) \times z$ the corresponding optical coordinates. n is the refractive index of the medium, α the semi-aperture angle, $k = 2\pi/\lambda$ and λ is the vacuum wavelength of light. The focal illumination intensity distribution is described by the I-PSF $h(\nu, u)$ and is calculated using vectorial diffraction theory [9]. $h(\nu, u)$ can be normalised to unity without affecting any conclusions on resolution or nonlinearity.

Modelling of the concept of repetitive excitation in scanning microscopy comes down to deriving the E-PSF of this system and the associated signal strength. The E-PSF describes the relative probability of detecting fluorescence from a dye molecule at a given point in the focal region [5,10]. For example, while for a single photon scanning excitation microscope the E-PSF is identical with the I-PSF, in nonresonant two-photon excitation microscopy, the E-PSF is given by $h_{\mathrm{E}}^{\mathrm{TPE}}(\nu,u) = [h(\nu/2,u/2)]^2$. The most common parameter for the lateral resolution of a far-field fluorescence microscope is the full width at half maximum (FWHM) of the EPSF, $h_{\mathrm{E}}(\nu,u)$ which, in conjunction with the attainable signal is a useful criterion of the spatial resolution.

In our model we use two pulses of different wavelengths, thus we will also have two I-PSFs, $h(\nu,u)$ and $h'(\nu,u)$ corresponding to the wavelength λ and λ' for the first and second pulse, respectively. For technical reasons, we define the ratio of the two wavelengths as $\varepsilon = \lambda/\lambda'$ and if both beams are focused by the same objective lens we can write $h'(\nu,u) = h(\varepsilon\nu,\varepsilon u)$. Taking into account that the energy gap $S_1 \rightarrow X_n$ is usually lower than that of $S_0 \rightarrow S_1$ we have $0.5 \leq \varepsilon \leq 1$. A value of $\varepsilon = 0.75$ was used throughout the paper.

The E-PSF of our microscope is given by the relative probability of a molecule to undergo $S_0 \rightarrow S_1$, which is the precondition for participating in the cycle between the higher states, times the probability that the molecule emits a fluorescence photon. Whereas the first probability is approximately proportional to $h(u,\nu)$, the second is given by $\eta(b,\Delta t)$. Using C as a constant normalising the E-PSF to unity we write

$$h_{\mathrm{eff}}(\nu,u,t) = Ch_1(\nu,u)\eta(b(\nu,u),t) = Ch_1(\nu,u)\eta(b_{\max}h(\varepsilon\nu,\varepsilon u),t)\,. \quad (13)$$

The function $h(\varepsilon\nu,\varepsilon u)$ weights the illumination intensity according to the three-dimensional diffraction pattern and $b_{\max}$ is the maximum intensity, found at $(\nu = 0, u = 0)$. The E-PSF is a function of time and expected to spatially shrink with elapsed time.

5 Evaluation of the microscope resolution and signal

$\eta(b,\Delta t)$ has a strong influence on the achievable resolution. We know from Figure 4, that for values of b above a certain level the re-excitation process will be saturated whereas for low values the process is not pronounced. To allow full exploitation of the whole nonlinear range $b_{\max}$ is selected to be higher than k_2.

To obtain an idea of how much the FWHM can be reduced we first study the effect on an arbitrary Gaussian lateral I-PSF $h(\nu) = \exp(-\nu^2)$ that is a function of the arbitrary variable ν with normalised FWHM $\Delta\nu_0 = 2\sqrt{\ln 2}$. If η is given by (7a) and assuming $b \gg k_2$, we have $\eta \cong \exp[-k_1k_2\Delta t/b] = \exp[-Ab_{\max}/b]$ with $A = k_1k_2\Delta t/b_{\max}$. For the FWHM $\Delta\nu$ of the E-PSF of such a beam the following equation holds:

$$\exp[-A\exp(\varepsilon^2(\Delta\nu/2)^2)]\exp[-(\Delta\nu/2)^2] \cong \frac{1}{2}\exp[-A]. \quad (14)$$

For large A we can determine the reduction in FWHM

$$\Delta\nu/\Delta\nu_0 \cong 1/\varepsilon\sqrt{A}\,. \quad (15)$$

This shows that theoretically the EPSF can be reduced to molecular scale albeit at a strong reduction of the signal. The probability that a molecule in the center of focus, which is initially excited, contributes to the fluorescence signal is given by

$$\eta = \exp[-(\Delta\nu_0/\Delta\nu)^2/\varepsilon^2]\,. \quad (16)$$

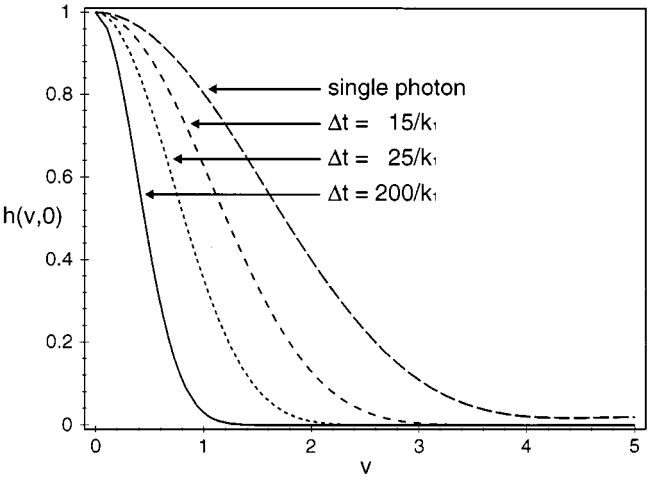

Fig. 5. Lateral profile of the E-PSF for a variety of delays and $b_{\max} = 50k_1$. The ratios of the decay rates are the same as in the previous figures. For even longer delays the FWHM could be further reduced albeit at a significant loss of signal.

Figure 5 displays the effective PSF now calculated using the more precise models for both the I-PSF and η as a function of the focal spatial coordinate ν with the temporal delay Δt as a parameter. The delays correspond to values of $A = 3$, 10 and 40 where the parameter $b_{\max} = 50k_1$ was chosen (see Figs. 3, 4). The FWHM is reduced by factors of 0.66, 0.47 and 0.25 which is only slightly less than expected from the approximation (15). Equation (16) overestimates the obtained signal by not more than a factor of 2.

As the effective resolution depends on both the spatial extent of the E-PSF and the obtained signal-to-noise ratio, we elect to calculate all resolution parameters for a fixed signal level, that is, we vary the other parameters of the model, $b_{\max}$ and Δt, but maintain a fixed fluorescence rate η. Figure 6 evaluates the lateral FWHM of the microscope with repetitive excitation for signal levels of $\eta = 0.05$, 0.2, 0.4, 0.6 as a function of the time window Δt. We also assumed $\theta = k_2/k_1 = 10$ and $\kappa = k_0/k_1 = 0.05$. The obtainable signal range is given by $\eta_0 = \exp(-k_1\Delta t) < \eta < \exp(-k_0\Delta t) = \eta_1$ thus theoretically limiting the range for Δt at a fixed signal level; the values η_0 and η_1 actually

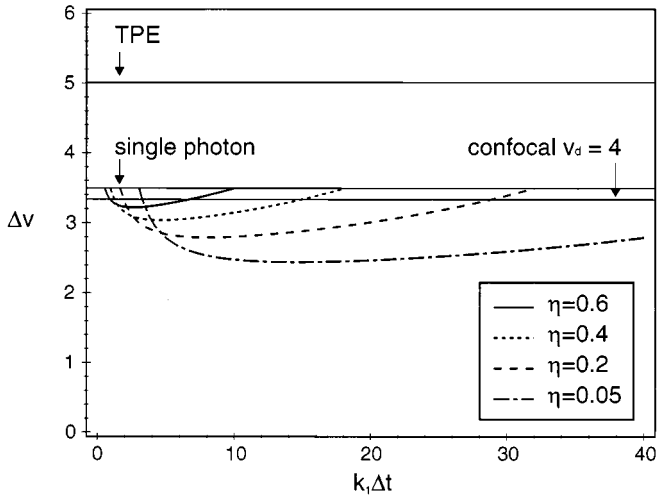

Fig. 6. The lateral FWHM of the E-PSF at fixed signal levels and varying combinations of maximum pump rate and delay. For optimum parameter values the lateral resolution is better than that of a confocal microscope and more than twice as good than that of a TPE microscope for all signal levels shown.

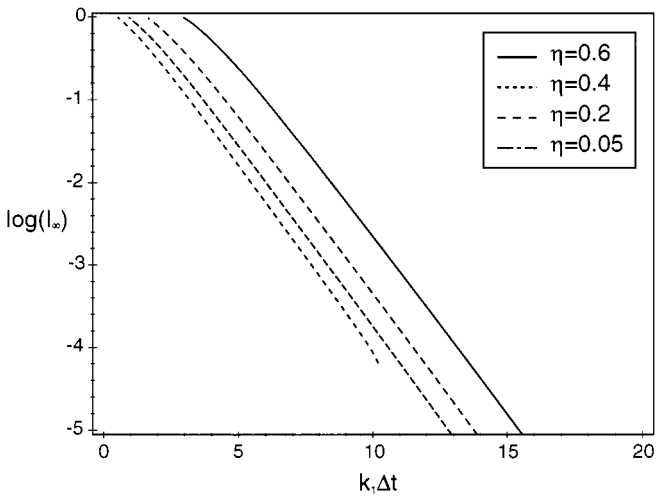

Fig. 7. The suppression of out-of-focus planes for fixed signal levels and varying combinations of maximum pump rate and delay; it is better than 5% for almost the whole range of values.

represent no and infinitely intense irradiation of the dye, respectively. At the boundaries no resolution effect can be achieved as the pump rate b loses its spatial dependence, as expected. A significant resolution increase is achieved within the boundaries, of course. The theoretical results are compared with those for a single photon excitation microscope operating at the same excitation wavelength, a confocal microscope with an Airy-disk sized pinhole of radius $\nu_d = 4$, and a nonresonant two-photon excitation microscope operating at the doubled wavelength. Figure 6 indicates that for the same, given signal at the focal point, a better resolution is achieved in our concept.

Besides calculating the lateral FWHM, we also investigate the response produced by an infinite fluorescent lateral plane scanned along the optic axis

$$I(u) = \frac{1}{C} \int \nu h_{\text{eff}}(\nu, u) \mathrm{d}\nu \,, \tag{17}$$

which is a decisive function for quantifying the axial resolution. C normalises the response to unity. In a microscope without 3D imaging capability, such as a conventional fluorescence microscope, the response $I(u)$ is a constant. In multiphoton and confocal microscopes for $u \to \infty$ we find $I_\infty(u) \to 0$. Generally I_∞ and the FWHM of $I(u)$, Δu, is a helpful criterion for the axial resolution.

For low intensity values, b, which occur at the outer focal region, $\eta(b,t)$ is linear. Therefore, in spite of the spatial reduction of the main maximum, there is always a residual linear background stemming from out-of-focus molecules which would be manifested as a constant signal of out-of-focus planes. In that case, for $u \to \infty$ we have $I(u) \to I_\infty > 0$. However, an appropriate parameter choice can reduce this background significantly. Figure 7 shows the numerical evaluation of I_∞ as a function of the time window Δt for the same signal levels and parameters

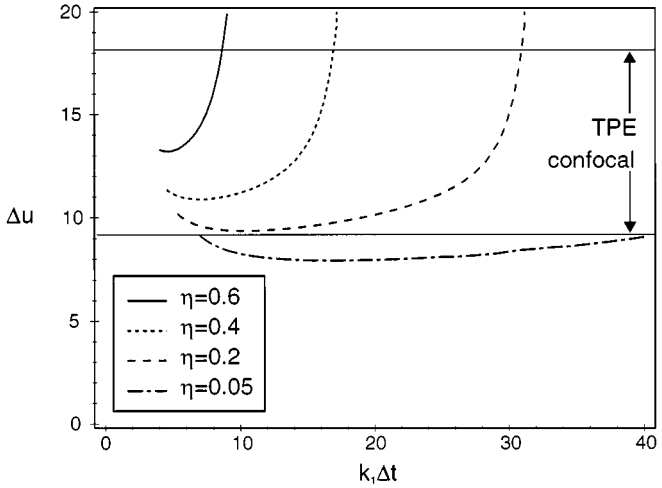

Fig. 8. The FWHM of the microscopes response to an infinite lateral fluorescent layer at the same signal levels as in the previous figures. At the expense of a fivefold decrease in signal the axial resolution of an ideal confocal microscope can be reached. This is twice the axial resolution of a microscope based on TPE when using the same dye.

used in the previous figure. In a large range of values for Δt, we obtain remarkable optical sectioning.

Figure 8 shows the FWHM of the z-response for the parameters η, the curves start at values where $I_\infty < 0.05$ is achieved, that is an out-of-focus suppression better than 5%. In principle, one could also allow a higher background and remove the background by subtraction at the cost of signal-to-noise ratio, as performed in other 3D imaging approaches [11]. Comparison with an ideal confocal microscope (pinhole size zero) shows that similar values for the z-resolution are obtained without the requirement of a confocal pinhole. The only microscope offering 3D resolution without confocal detection is based on nonresonant multiphoton excitation. Its resolution is improved by a

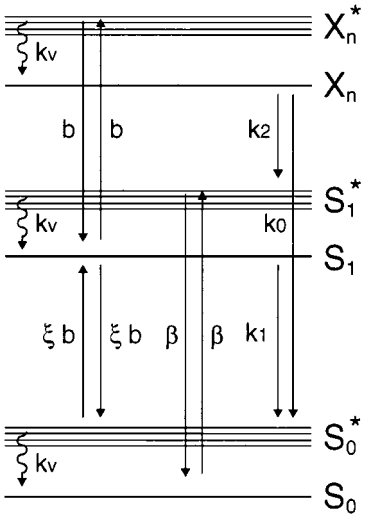

Fig. 9. Jablonski diagram of the model incorporating stimulated emission. The vibrational states, from which stimulated emission takes place, decay at a fast rate k_ν into the electronic levels. Further stimulated emission from the first excited state could take place due to the longer wavelength irradiation from the second laser. It is proportional to the pump rate into the highest state.

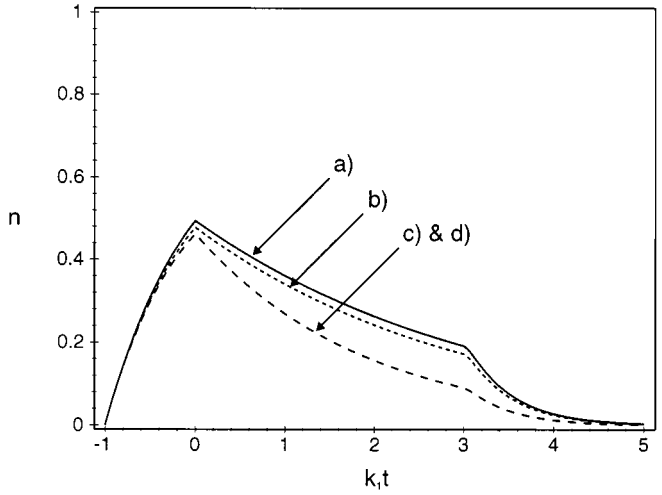

Fig. 10. Time evolution of the total probability of the dye to be electronically excited for a) no stimulated emission, *e.g.* infinite decay rates of the vibrational levels, b) vibrational decay at a rate $k_\nu = 100k_1$. Graphs c) and d) represent model calculations for stimulated emission from the first excited singlet state, and the case of a leak k_0, respectively. For the assumed rate both curves almost coincide as predicted in the text.

factor of more than two in both lateral and axial directions by our model.

Finally we want to examine the influence of two additional parameters. One is stimulated emission from the first excited singlet state. The rate of this process would be a fraction ξb of the pump rate. The proportionality constant indicates how many dyes are sent into their ground state instead of going through an additional excitation-decay cycle. In this it is very similar to the "leak" $X_n \rightarrow S_0$ and further analysis shows, indeed, that the effects are almost identical if $k_0 \cong k_2\xi$.

If pump rates become large, then stimulated emission from vibrational levels might play a role. Let the rate at which the vibrational levels decay be denoted by k_ν. For the analysis of both effects we extended the model as shown in Figure 9. For every set of the rates the eigenvalues of the resulting matrix were found numerically by triagonalising it and the eigenvectors were then determined through singular value decomposition (data not shown). The time evolution of the now 6-dimensional vector n can then be described using exponential functions.

We are interested in the sum of the populations of all electronically excited states. Figure 10 compares its time evolution starting from the initial excitation. The solid line a) represents the graph for the parameters used throughout the paper. In graphs c) and d), we compared the effect of stimulated emission from the first excited state with that of an assumed leak rate enlarged to $k_0 \rightarrow k_0 + \xi k_2$. As predicted the curves proved to be indistinguishable. Graph b) shows the time evolution when vibrational levels decay, at a rate of $k_\nu = 100k_1$, into states from where stimulated emission is impossible. The form of the graph is conserved and the relative changes are slight even for this slow rate confirming our view that stimulated emission from the vibrational levels can be ignored in our considerations.

6 Discussion and conclusion

We have investigated the concept of repeatedly exciting a fluorescent system in order to generate a nonlinear fluorescence signal and improved spatial resolution in far-field microscopy. For dyes adequately described by a three-state model we quantified the achievable nonlinearity as a function of the relaxation and pump rates between the various energy states. In this case a strong nonlinear dependence of the fluorescence on the illumination intensity can be achieved, based on linear properties of the fluorophore alone. The model assumes two excited states, namely a lower, fluorescent state and a second excited state to which the molecules can be transferred for a short time in order to cause a temporal delay in the fluorescence decay. The nonlinear signal is extracted by applying a temporal filter. The most prominent choice for the dye seems to be an organic molecule, although most standard organic fluorophores may well prove to be insufficiently photostable. However, we note that our study applies to any fluorescent system featuring a state allowing for a delay. Recent research activities in fluorescent probe synthesis [12] encourage the view that future developments may yield a fluorescent systems meeting the above requirements or could be directed along the lines indicated in our model.

In contrast to nonresonant multiphoton excitation, the nonlinearity gained by repeated excitation leads to a genuine reduction of the effective focal area of a scanning light microscope. The nonlinearity can in principle be increased

indefinitely and the theoretical resolution of a scanning microscope could consequently reach molecular dimensions, however, for vanishing signals. The signal tradeoff seems common to all resolution-improving techniques, including near-field optics, so a significant increase of the obtainable fluorescence signal is an issue of tantamount importance in microscopy. Nevertheless, a comparison at *equal* signal levels shows that the resolution predicted by the concept of repetitive excitation would be substantially increased over a standard two-photon or confocal fluorescence microscope. Successful implementation of the concept would thus provide inherent three-dimensional, multiphoton imaging without recourse to higher-order susceptibilities of the material.

References

1. J. Pawley, *Handbook of Biological Confocal Microscopy* (Plenum Press, New York, 1995); C.J.R. Sheppard, D.M. Shotton, *Confocal Laser Scanning Microscopy* (Bios Scientific Publishers, Oxford, 1997).
2. W. Denk, J.H. Strickler, W.W. Webb, Science **248**, 73 (1990).
3. S.W. Hell, K. Bahlmann, M. Schrader, *et al.*, J. Biomed. Opt. **1**, 71 (1996); D.L. Wokosin, V. Centonze, J.G. White, *et al.*, IEEE J. Sel. Top. Quant. Electron. **2**, 1051 (1996).
4. C.J.R. Sheppard, M. Gu, Optik **86**, 104 (1990), erratum **92**, 102 (1992); S. Hell, E.H.K. Stelzer, Opt. Commun. **93**, 277 (1992).
5. S. Hell, Opt. Commun. **106**, 19 (1994).
6. F.P. Schäfer (editor), *Dye Lasers* (Springer, Berlin, Heidelberg, 1973).
7. K. Sasaki, M. Koshioka, H. Masuhara, J. Opt. Soc. Am. A **9**, 932 (1992).
8. S. Speiser, N. Shakkour, Appl. Phys. B **38**, 191 (1985); S. Speiser, R.v.d. Werf, J. Kommandeur, Chem. Phys. **1**, 297 (1973).
9. B. Richards, E. Wolf, Proc. Roy. Soc. Lond. A **253**, 358 (1959); C.J.R. Sheppard, H.J. Matthews, J. Opt. Soc. Am. A **4**, 1354 (1987).
10. S.W. Hell, in *Topics in Fluorescence Spectroscopy*, edited by J.R. Lakowicz (Plenum Press, New York, 1997), Vol. 5, p. 361.
11. M.A.A. Neil, R. Juskaitis, T. Wilson, Opt. Lett. **22**, 1905 (1997).
12. W.C.W. Chan, S. Nie, Science **281**, 2016 (1998); M. Bruchez jr., M. Moronne, P. Gin, *et al.*, Science **281**, 2013 (1998).